Pore Filling of Nanostructured Electrodes in Dye Sensitized Solar Cells by Initiated Chemical Vapor Deposition

ARTICLE *in* NANO LETTERS · FEBRUARY 2011

Impact Factor: 13.59 · DOI: 10.1021/nl103020w · Source: PubMed

2 AUTHORS:

Siamak Nejati
Yale University
38 PUBLICATIONS **231** CITATIONS
SEE PROFILE

Kenneth Lau
Drexel University
72 PUBLICATIONS **2,351** CITATIONS
SEE PROFILE

NANO LETTERS

LETTER

pubs.acs.org/NanoLett

Pore Filling of Nanostructured Electrodes in Dye Sensitized Solar Cells by Initiated Chemical Vapor Deposition

Siamak Nejati and Kenneth K. S. Lau*

Department of Chemical and Biological Engineering, Drexel University, 3141 Chestnut Street, Philadelphia, Pennsylvania 19104, United States

Supporting Information

ABSTRACT: The dye sensitized solar cell (DSSC) operation depends on a liquid electrolyte. To achieve better performance, the liquid should be replaced with a solid or gel electrolyte, e.g., polymers. Here, we demonstrate initiated chemical vapor deposition as an effective liquid-free means for in situ polymerization and pore filling. We achieve complete pore filling of 12 μm thick titania resulting in enhanced cell performance that is attributed to reduced charge recombination at the electrolyte−electrode interface.

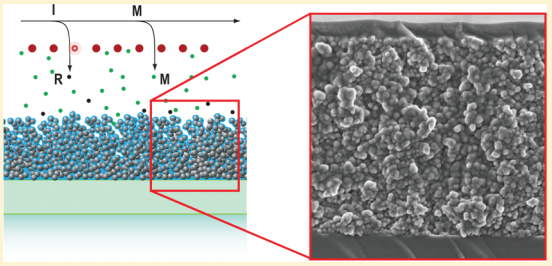

KEYWORDS: Dye sensitized solar cell, initiated chemical vapor deposition (iCVD), poly(2-hydroxyethyl methacrylate), mesoporous titanium dioxide, pore filling

Since the seminal report of O'Regan and Grätzel[1] on the dye sensitized solar cell, the dye sensitized solar cell (DSSC) has shown increasing potential as a viable photovoltaic technology for harvesting sunlight. In the DSSC, the mesoscopic structure of the titanium dioxide electrode plays a significant role in increasing cell efficiency by providing the photosensitizer dye with much greater surface area for light harvesting.[2] Although this device architecture provides a workable efficiency, the presence of a redox couple in a liquid electrolyte to regenerate the dye presents practical challenges.[3−5] Sealing in of the liquid to prevent leakage and evaporation becomes an overbearing issue, so replacing the liquid electrolyte is critical for enhancing the operability and durability of the cell. Organic and inorganic solid state hole transport materials,[6−8] conjugated polymers,[9,10] and solid and gel polymer electrolytes[11−14] have been explored to replace the liquid electrolyte. However, infiltrating solid materials into the mesoporous TiO_2 structure remains a major obstacle as many methods do not provide complete pore filling of the electrode.[4,15] Although the importance of pore filling and pore wetting is recognized as a necessary technological leap for advancing DSSC performance, currently the effective electrode thickness of the device fabricated with these materials has been limited by their penetration depth into the mesoporous TiO_2 layer to ~2 μm.[16−18] The nanoscale pore diameter and narrow pore structure make it especially difficult for liquid-based techniques to transport these materials due to viscous and steric effects. In addition, these processes introduce solvents into the system that make their complete removal nontrivial, and the presence of any unwanted chemical will most likely deteriorate cell performance.

Here, we present initiated chemical vapor deposition (iCVD) as a solvent-free technique with its ability to form solid polymers in nanoscale structures as an effective route for crossing the DSSC technological hurdle.[19−21] iCVD is an adsorption limited process that relies on the transport of gaseous monomer and activated initiator to the surface that is followed by a surface chemical reaction. By enabling polymerization and deposition in a single step, iCVD offers physical control at the nanoscale[22−25] and chemical control over synthesis pathways[26−28] (including copolymerization and cross-linking) needed for device fabrication. We take advantage of this unique method to polymerize poly(2-hydroxyethyl methacrylate) (PHEMA) as a potential polymer electrolyte material inside the mesoporous TiO_2 electrode of the DSSC; see Figure 1. PHEMA has been chosen as the presence of the ester and hydroxyl groups are expected to facilitate ion transport and enable the formation of a stable gel electrolyte with ethylene and propylene carbonate typically used as dielectrics in DSSCs.[29] Using conventional free radical polymerization of 2-hydroxyethyl methacrylate (HEMA) and *tert*-amyl peroxide (TAPO) as monomer and initiator, respectively, we have investigated the effect of critical iCVD parameters in influencing the rate of polymer formation inside the pores in order to obtain a systematic way for filling the mesoscopic TiO_2 electrode effectively. The fabricated DSSC integrating iCVD PHEMA as a quasi solid state polymer electrolyte shows enhanced performance compared with a standard liquid filled DSSC. See Supporting Information for experimental details.

To obtain pore filling of the mesoporous TiO_2 electrode with PHEMA, we performed iCVD on 3−4 μm thick electrode layers

Received: August 25, 2010
Revised: November 29, 2010
Published: December 20, 2010

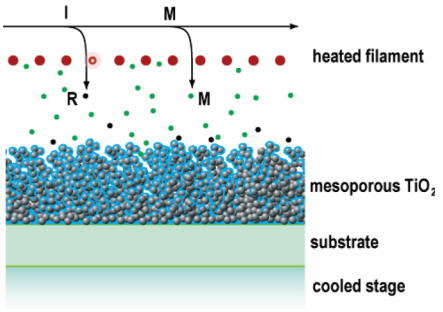

Figure 1. Schematic of the pore filling process during initiated chemical vapor deposition (iCVD). Monomer (M) and initiator (I) molecules are delivered into the reaction chamber in the form of gaseous vapors. The initiator is selectively activated by a series of heated filaments. The activated initiator (R) and monomer (M) adsorb onto the TiO_2 surface within the nanostructured mesoporous electrode that is kept cooled to enhance the adsorption-limited process. Addition polymerization of the monomer at activated initiator sites results in the formation of a growing polymer inside the pores.

to systematically investigate different iCVD parameters and observe the resulting electrode scanning electron microscopy (SEM) cross sections. Total reactor pressure was increased from 60 to 200 mTorr, essentially to see the effect of system pressure on the amount of PHEMA polymer which has filled the pores during iCVD (all other conditions remained constant, with HEMA, TAPO, and N_2 flow rates each set at 0.4 sccm). Compared to a clean cross section of mesoporous TiO_2 before iCVD (Figure 2a), deposition at 60 mTorr yields only a polymer coating forming on top of the electrode without any polymer being visible within the porous network (Figure 2b). As total pressure increases above 80 mTorr, filling of the inner pore volume starts taking place (not shown). At 125 mTorr, a completely pore filled cross section together with a top overcoat is observed (Figure 2c). Further increase in total pressure to 200 mTorr results in the quality of fill deteriorating again, with evidence of partial filling within the mesoporous layer and premature coating on top (Figure 2d). To separate the individual effects of monomer and initiator partial pressures on pore filling, each reactant flow rate was varied while keeping the other constant and compensating with nitrogen inert to maintain a constant total flow rate (1.2 sccm) at a fixed total pressure (125 mTorr). Considering the initiator, adjusting TAPO flow rate from 0.2 to 0.8 sccm reveals that flows above 0.4 sccm give complete pore filling while lower flows yield partial filling with greater filling fraction as flow increases (Figure S1 in the Supporting Information). This is to be expected since the initiator contributes to the amount of initiated polymer chain radicals, and once sufficient initiator concentration has been reached, polymer growth becomes monomer limited. This trend has been observed previously with iCVD polymerization of acrylate and methacrylate polymers.[30−32] Likewise, considering the monomer, adjusting the flow rate between 0.2 and 0.6 sccm (while keeping a fixed total flow of 1.2 sccm and total pressure of 125 mTorr) shows that the fill quality initially improves with increasing monomer flow rate, and after passing a fully filled state, pore filling deteriorates again (Figure S1 in the Supporting Information). This observation indicates that pore filling is much more sensitive to the monomer than to the initiator flow rate. As an important note, although the initiator and monomer flows and their gas concentrations are comparable (which might suggest long chain

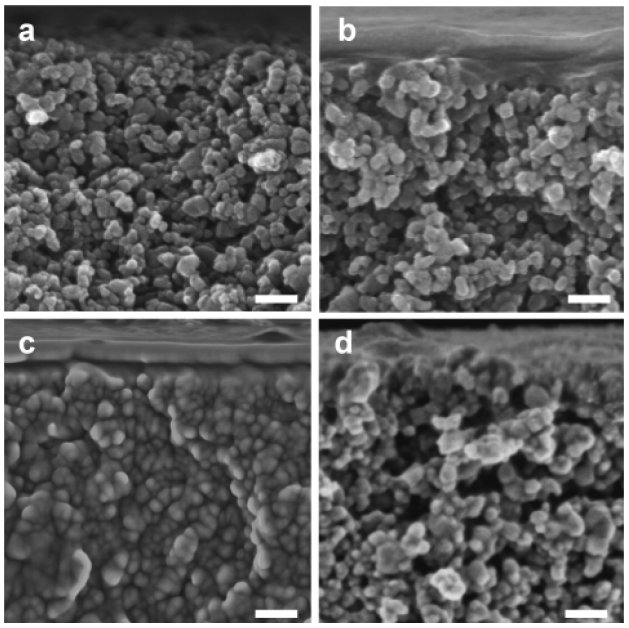

Figure 2. Effect of total pressure on pore filling, showing cross sectional SEM of the 4 μm thick TiO_2 electrodes that are (a) uncoated, and after iCVD treatment at total pressures of (b) 60, (c) 125, and (d) 200 mTorr (scale bar = 100 nm). Complete pore filling is observed at intermediate pressures.

polymer formation would not be possible), the surface concentration based on surface adsorption of the initiator is actually much lower than for the monomer due to its higher vapor pressure (by a factor of 10). In addition, the initiator is activated in the gas phase, so we would expect only a fraction of the activated initiator to actually reach the surface.

Thus, we attribute the observed complete pore filling at intermediate total pressures (Figure 2) to mainly the effect of the monomer. To explain this pore filling behavior, we consider the process to be composed of three main steps: (1) diffusion of the reactants inside the mesoporous structure; (2) adsorption and surface diffusion of the reactants; and (3) polymerization reaction at the surface. Like all porous media, we expect mass transport and reaction kinetics to each play a critical role in polymer growth inside the pores. Diffusion needs to take into account both gas and surface diffusion. Under iCVD conditions in mesoporous TiO_2, Knudsen diffusion dominates gas phase transport (Knudsen number $Kn = \lambda/d_{pore} \sim 10^4$, where λ and d_{pore} are estimated to be 160 μm and 17 nm, respectively). Surface diffusion, on the other hand, requires an understanding of the adsorption behavior within mesoporous materials, and experimental studies have shown that surface diffusivity reaches a maximum at some intermediate surface coverage of the adsorbate,[33,34] a clue that this phenomenon might capture the observed trend in our work. Thus, here an effective diffusion coefficient (D_{eff}) has been determined by considering gas and surface diffusion acting as parallel resistances to transport. This allows us to estimate the diffusion time constant ($\tau_D = L^2/D_{eff}$, where L is the mesoporous layer thickness) which varies with surface coverage or equivalently the relative pressure of the monomer ($z = P_M/P_{M,sat}$). Likewise, a reaction time constant ($\tau_R = 1/k_p[M]$, where k_p is the propagation rate constant for polymerization and [M] is the surface concentration of monomer) has been calculated that also changes with z (see Supporting Information

dx.doi.org/10.1021/nl103020w |*Nano Lett.* 2011, 11, 419–423

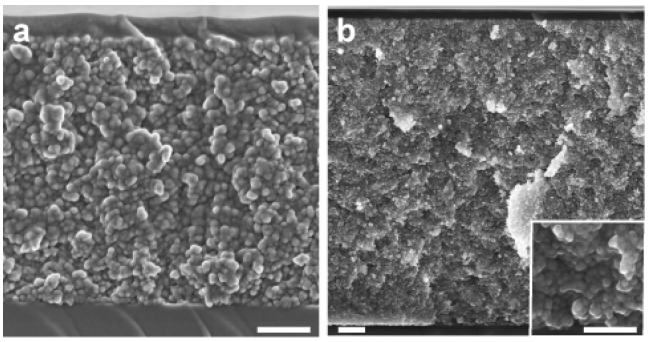

Figure 3. Pore filling of TiO_2 electrodes of different thicknesses of (a) 4 μm (scale bar = 500 nm), and (b) 12 μm (scale bar = 1 μm), the inset shows the bottom of the sample (scale bar = 500 nm). By carefully controlling mass transport (gas and surface diffusion) and surface reaction kinetics, complete pore filling can be achieved with iCVD.

for more details). Plots of τ_D and τ_R as a function of z then indicate whether mass transport or reaction is rate limiting. As described in Figure S2 in the Supporting Information, there is a sweet spot at intermediate z values in which the reaction becomes limiting ($\tau_R > \tau_D$), and it is within this range of monomer partial pressure (P_M = 25−65 mTorr, $0.03 < z < 0.09$) that we see complete pore filling of the mesoporous TiO_2 electrode (Figure 2c). At either lower or higher monomer concentrations, pore diffusion becomes limited, and this leads to a lack of polymer growth within the pores and premature formation of a top overcoat (Figure 2b,d). With this knowledge, we are able to control iCVD conditions to achieve complete pore filling successfully for electrode thicknesses up to 12 μm (Figure 3), which is much thicker than is possible with other reported procedures (~2 μm).[16,17,35,36] As a more quantitative means of measuring pore filling, cross sectional SEM was complemented with thermogravimetric analysis (TGA) to estimate the amount of polymer that was grown inside the mesopores. As shown in Figure S3 in the Supporting Information, the percent pore filling is defined as the percent of the total pore volume available initially in the mesoporous TiO_2 electrode which has been grown with polymer during iCVD polymerization. The porosity (43−45%) and total available pore volume were derived from N_2 sorption measurements while the polymer volume was deduced from TGA thermograms (Figure S4 in the Supporting Information). On the basis of these calculations, the percent pore filling for example is estimated to be in the range of 92−100% for the thickest 12 μm electrode, with the uncertainty in the value coming from the sensitivity range and variability of the various measurements (see Supporting Information for more details). As mentioned earlier, pore filling of the DSSC mesoporous electrode remains a technological hurdle which has significantly limited the use of the solid materials in these devices. iCVD therefore represents an attractive means for incorporating polymer electrolyte in the fabrication of DSSCs.

Once proper conditions for pore filling were found, we applied iCVD and integrated PHEMA as a polymer electrolyte in the dye sensitized TiO_2 electrode. After incorporating the iodide−triiodide redox couple in 50:50 propylene carbonate and γ-butyrolactone and assembling into a complete quasi solid state DSSC, photocurrent−voltage measurements were made and compared with a standard liquid electrolyte cell containing acetonitrile. As shown in Figure S5 in the Supporting Information, although the short circuit current (J_{sc}) of the polymer electrolyte DSSC is reduced, the open circuit voltage (V_{oc}) is notably higher when compared with the acetonitrile liquid

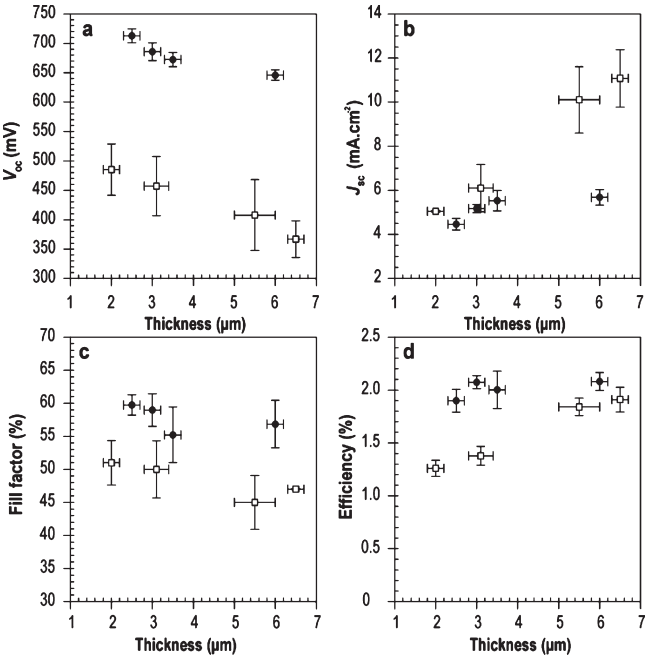

Figure 4. Comparison between the performance of DSSCs fabricated with a quasi solid state PHEMA polymer electrolyte containing 50:50 vol % propylene carbonate and γ-butyrolactone (●), and with a standard liquid electrolyte containing acetonitrile (□) for different TiO_2 thicknesses, showing (a) open circuit voltage V_{oc}, (b) short circuit current J_{sc}, (c) fill factor FF, and (d) power conversion efficiency η (error bar = 1 SD). Polymer electrolyte DSSCs provide similar efficiency as the liquid electrolyte cells with TiO_2 electrode thicknesses that are nearly three times thinner.

electrolyte cell. This behavior is observed with ruthenium-based photosensitizer dyes 535 (N3) and 505, although the remainder of our discussion will focus on DSSCs incorporating the more effective dye 535. To further elucidate the effect of PHEMA pore filling, we investigated the changes in DSSC performance with increasing TiO_2 thickness and again made comparisons between polymer electrolyte and acetonitrile liquid electrolyte cells, as detailed in Figure 4. On the basis of current−voltage measurements, power conversion efficiency η of each cell has been derived from J_{sc} and V_{oc} as well as its fill factor, FF, defined as the ratio of the actual maximum power to the theoretical derivable power (i.e., $J_{sc}V_{oc}$). Knowing the power density of the illuminated light (W_o), cell efficiency has been calculated as $\eta = (FF)J_{sc}V_{oc}/W_o$. As expected, the standard liquid cell shows a considerably smaller V_{oc} with thicker electrodes, which is typically attributed to an increase in recombination sites for the redox couple (triiodide) to recapture dye-injected electrons from the TiO_2 as more surface area is available.[37,38] Similarly, the increase in surface area with thicker electrodes leads to higher J_{sc} in the liquid cell with the greater amount of photosensitization. In contrast, for the completely pore filled polymer electrolyte cell, V_{oc} and J_{sc} appear to be less sensitive to electrode thickness especially as electrode thickness increases above 4 μm. The smaller effect on V_{oc} could be due to passivation of the TiO_2 surface when in contact with the iCVD polymer as has been observed with small molecules.[39] However, it is clearly evident that V_{oc} is consistently much higher for the polymer cell compared to the liquid one at all electrode thicknesses we tested. There seems to be a leveling off of J_{sc}, which suggests some

dx.doi.org/10.1021/nl103020w |*Nano Lett.* 2011, 11, 419–423

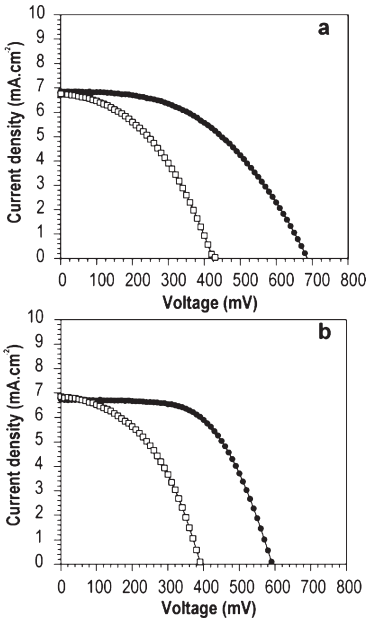

Figure 5. Effect of redox solvent on the performance of DSSCs fabricated with the polymer electrolyte (●) and the corresponding liquid electrolyte (□) containing (a) 50:50 vol % propylene carbonate and γ-butyrolactone and (b) pure propylene carbonate. In each case, V_{oc} is enhanced while J_{sc} remains relatively unchanged in the polymer electrolyte cell.

saturation effect, and could be a result of an increase in diffusion resistance to ion conduction of the redox couple within the polymer matrix. This is supported by a similar trend we observe when the redox concentration was lowered to a point where changes in J_{sc} with illuminated light intensity (at constant electrode thickness) reach a plateau (Figure S6 in the Supporting Information). Since this behavior is only observed in the polymer electrolyte cell, the trends suggest charge transport rather than charge generation becomes limiting, see Supporting Information for more details. In Figure 4, although J_{sc} is lower, the significantly higher V_{oc} together with a relatively constant FF yield higher device efficiency for the polymer electrolyte cell compared with the liquid acetonitrile cell at all the electrode thicknesses considered. In fact, the polymer cell efficiencies remain fairly constant as a result of a lack of sensitivity of the device parameters. Significantly, the DSSC integrating the iCVD PHEMA electrolyte can provide similar efficiency as the acetonitrile liquid electrolyte DSSC using TiO_2 electrodes that are nearly a factor of 3 thinner (as an important note, the difference in efficiencies observed between the polymer and liquid electrolyte cells is solely due to the replacement of the liquid with the polymer, and there has been no attempt to fully optimize cell performance). Importantly, this implies that there could be potential advantages when we consider a similar factor in reducing materials usage, especially of the expensive dye, as well as the possibility of greater cell robustness, particularly when thinking of applying the cell architecture on flexible substrates.

To further understand the resulting V_{oc} enhancement in the polymer electrolyte DSSC, we compared the current−voltage characteristics of this cell with liquid cells containing the same redox solvent rather than acetonitrile. As shown in Figure 5, when either a 50:50% of propylene carbonate and γ-butyrolactone or pure propylene carbonate was used to incorporate the

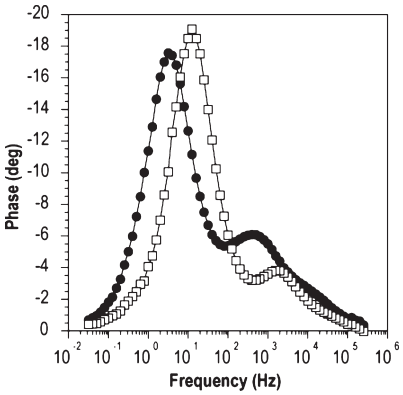

Figure 6. Comparison between the Bode diagrams at their respective V_{oc} of DSSCs fabricated with the polymer electrolyte (●) and the corresponding liquid electrolyte (□) containing propylene carbonate. The shift of the midfrequency peak to lower frequency of the polymer electrolyte cell indicates a decrease in charge recombination at the electrolyte−electrode interface.

iodide−triiodide redox couple, we see that J_{sc} does not change significantly between the liquid and polymer electrolyte cells using the same redox solvent as it does between the acetonitrile and polymer electrolyte cells. In contrast, V_{oc} is again consistently higher in both cases for the polymer cell when compared with their liquid counterparts. This implies that since J_{sc} is not affected, the increase in V_{oc} cannot have come from a difference in ion conduction as a result of changing from a liquid to a quasi solid state polymer electrolyte. We further compared polymer cells with complete fill (cf. Figure 2c) and partial fill showing premature blockage (cf. panels b and d of Figure 2). As shown in Figure S7 in the Supporting Information, the partially filled polymer cell again shows little change in J_{sc} while the increase in V_{oc} is now much smaller than if the electrode were completely filled. This demonstrates the need for complete pore filling to derive the maximum benefit of the polymer electrolyte in enhancing DSSC performance as a result of the largest gain in V_{oc}.

We therefore performed electrochemical impedance spectroscopy on the polymer and liquid cells at their respective V_{oc} to gain further insight. Figure 6 shows the Bode plots of the polymer and liquid electrolyte DSSCs containing propylene carbonate and illuminated under 1 sun corresponding to global AM 1.5 and 100 mW/cm^2 irradiance. We observe a shift in the midfrequency peak toward lower frequency when the liquid electrolyte is replaced with the polymer. This spectral peak frequency is a measure of the recombination time constant of the electrons with the redox couple[40] (triiodide) if we assume that charge recombination with the oxidized dye molecules can be neglected due to fast reduction of the dye through the redox couple.[41] Thus, the shift to lower frequency suggests an increase in effective electron lifetime from ~12 ms in the liquid cell to ~50 ms in the polymer electrolyte cell due to reduced recombination with the electrolyte. We believe this decrease in charge recombination is the cause for the substantially higher V_{oc}. It is reasonable to expect that the contact of the quasi solid polymer with the TiO_2 electrode surface through complete pore filling can alter interfacial properties. For example, charge transfer via surface trap states could be reduced by the polymer blocking active sites on the TiO_2 surface.[42] Also, it is possible that Li^+ ions (from the redox species) could coordinate with the polymer matrix thereby

dx.doi.org/10.1021/nl103020w |*Nano Lett.* 2011, 11, 419–423

limiting lithium adsorption on the TiO_2 surface, which would result in band edge movement and consequently an increase in V_{oc} of the cell.[43]

In summary, we have successfully utilized iCVD to integrate a polymer electrolyte into the mesoporous TiO_2 electrode of the DSSC. By careful control of the diffusion transport and surface kinetics during iCVD, complete pore filling can be obtained. This results in significant enhancement in cell properties. The efficiency of the quasi solid state PHEMA electrolyte DSSC is higher when compared with their liquid electrolyte counterparts. We attribute the observed increase in open circuit cell voltage to the suppression of electron recombination at the electrolyte—electrode interface as a result of the exceptional pore filling achieved by iCVD. iCVD promises to be a valuable synthesis and processing pathway which as demonstrated here has the potential to overcome the major technological constraint of using a liquid electrolyte in the DSSC.

■ ASSOCIATED CONTENT

Supporting Information. Experimental details on iCVD polymerization, polymer electrolyte characterization, pore filling estimation, solar cell preparation, and photovoltaic measurements and more detailed accounts on the effect of individual reactant on pore filling, the effect of monomer transport, and reaction on pore filling, pore filling calculations, the effect of photosensitizer dye on DSSC performance, the diffusion limitation on photocurrent density, and the effect of partial pore filling on DSSC performance. This material is available free of charge via the Internet at http://pubs.acs.org.

■ AUTHOR INFORMATION

Corresponding Author
*E-mail: klau@drexel.edu.

■ ACKNOWLEDGMENT

This work has been supported by the NSF CAREER Award (CBET-0846245), NSF SGER Grant (CBET-0820608), and ACS PRF Grant (48160-G5). We also acknowledge the use of Drexel University's Centralized Research Facilities.

■ REFERENCES

(1) O'Regan, B.; Grätzel, M. *Nature* **1991,** *353*, 737–740.
(2) Grätzel, M. *J. Photochem. Photobiol., A* **2004,** *164*, 3–14.
(3) Wang, P.; Zakeeruddin, S. M.; Moser, J. E.; Nazeeruddin, M. K.; Sekiguchi, T.; Grätzel, M. *Nat. Mater.* **2003,** *2*, 402–407.
(4) Matsumoto, M.; Miyazaki, H.; Matsuhiro, K.; Kumashiro, Y.; Takaoka, Y. *Solid State Ionics* **1996,** *89*, 263–267.
(5) de Freitas, J. N.; Nogueira, A. F.; De Paoli, M. A. *J. Mater. Chem.* **2009,** *19*, 5279–5294.
(6) Bach, U.; Lupo, D.; Comte, P.; Moser, J. E.; Weissortel, F.; Salbeck, J.; Spreitzer, H.; Grätzel, M. *Nature* **1998,** *395*, 583–585.
(7) Meng, Q. B.; Takahashi, K.; Zhang, X. T.; Sutanto, I.; Rao, T. N.; Sato, O.; Fujishima, A.; Watanabe, H.; Nakamori, T.; Uragami, M. *Langmuir* **2003,** *19*, 3572–3574.
(8) Kruger, J.; Plass, R.; Grätzel, M.; Matthieu, H. J. *Appl. Phys. Lett.* **2002,** *81*, 367–369.
(9) Gebeyehu, D.; Brabec, C. J.; Sariciftci, N. S. *Thin Solid Films* **2002,** *403*, 271–274.
(10) Saito, Y.; Fukuri, N.; Senadeera, R.; Kitamura, T.; Wada, Y.; Yanagida, S. *Electrochem. Commun.* **2004,** *6*, 71–74.
(11) Cao, F.; Oskam, G.; Searson, P. C. *J. Phys. Chem.* **1995,** *99*, 17071–17073.
(12) Nogueira, A. F.; Durrant, J. R.; De Paoli, M. A. *Adv. Mater.* **2001,** *13*, 826–830.
(13) Wu, J. H.; Lan, Z.; Lin, J. M.; Huang, M. L.; Hao, S. C.; Sato, T.; Yin, S. *Adv. Mater.* **2007,** *19*, 4006–4011.
(14) Komiya, R.; Han, L. Y.; Yamanaka, R.; Islam, A.; Mitate, T. *J. Photochem. Photobiol., A* **2004,** *164*, 123–127.
(15) Snaith, H. J.; Humphry-Baker, R.; Chen, P.; Cesar, I.; Zakeeruddin, S. M.; Grätzel, M. *Nanotechnology* **2008,** *19*, No. 240300.
(16) Schmidt-Mende, L.; Grätzel, M. *Thin Solid Films* **2006,** *500*, 296–301.
(17) O'Regan, B.; Lenzmann, F.; Muis, R.; Wienke, J. *Chem. Mater.* **2002,** *14*, 5023–5029.
(18) Yum, J. H.; Chen, P.; Grätzel, M.; Nazeeruddin, M. K. *ChemSusChem* **2008,** *1*, 699–707.
(19) Tenhaeff, W. E.; Gleason, K. K. *Adv. Funct. Mater.* **2008,** *18*, 979–992.
(20) Baxamusa, S. H.; Im, S. G.; Gleason, K. K. *Phys. Chem. Chem. Phys.* **2009,** *11*, 5227–5240.
(21) Asatekin, A.; Barr, M. C.; Baxamusa, S. H.; Lau, K. K. S.; Tenhaeff, W.; Xu, J. J.; Gleason, K. K. *Mater. Today* **2010,** *13*, 26–33.
(22) Im, S. G.; Bong, K. W.; Lee, C. H.; Doyle, P. S.; Gleason, K. K. *Lab Chip* **2009,** *9*, 411–416.
(23) Lau, K. K. S.; Gleason, K. K. *Adv. Mater.* **2006,** *18*, 1972–1977.
(24) Gupta, M.; Kapur, V.; Pinkerton, N. M.; Gleason, K. K. *Chem. Mater.* **2008,** *20*, 1646–1651.
(25) Lau, K. K. S.; Bico, J.; Teo, K. B. K.; Chhowalla, M.; Amaratunga, G. A. J.; Milne, W. I.; McKinley, G. H.; Gleason, K. K. *Nano Lett.* **2003,** *3*, 1701–1705.
(26) Tenhaeff, W. E.; Gleason, K. K. *Thin Solid Films* **2009,** *517*, 3543–3546.
(27) Lau, K. K. S.; Gleason, K. K. *Thin Solid Films* **2008,** *516*, 678–680.
(28) O'Shaughnessy, W. S.; Mari-Buye, N.; Borros, S.; Gleason, K. K. *Macromol. Rapid Commun.* **2007,** *28*, 1877–1882.
(29) Yang, H.; Huang, M.; Wu, J.; Lan, Z.; Hao, S.; Lin, J. *Mater. Chem. Phys.* **2008,** *110*, 38–42.
(30) Lau, K. K. S.; Gleason, K. K. *Macromolecules* **2006,** *39*, 3695–3703.
(31) Ozaydin-Ince, G.; Gleason, K. K. *Chem. Vap. Deposition* **2010,** *16*, 100–105.
(32) Baxamusa, S. H.; Gleason, K. K. *Chem. Vap. Deposition* **2008,** *14*, 313–318.
(33) Choi, J. G.; Do, D. D.; Do, H. D. *Ind. Eng. Chem. Res.* **2001,** *40*, 4005–4031.
(34) Valiullin, R.; Kärger, J.; Gläser, R. *Phys. Chem. Chem. Phys.* **2009,** *11*, 2833–2853.
(35) Ding, I. K.; Tetreault, N.; Brillet, J.; Hardin, B. E.; Smith, E. H.; Rosenthal, S. J.; Sauvage, F.; Gratzel, M.; McGehee, M. D. *Adv. Funct. Mater.* **2009,** *19*, 2431–2436.
(36) Bartholomew, G. P.; Heeger, A. J. *Adv. Funct. Mater.* **2005,** *15*, 677–682.
(37) Nelson, J.; Chandler, R. E. *Coord. Chem. Rev.* **2004,** *248*, 1181–1194.
(38) Ito, S.; Zakeeruddin, S. M.; Humphry-Baker, R.; Liska, P.; Charvet, R.; Comte, P.; Nazeeruddin, M. K.; Pechy, P.; Takata, M.; Miura, H.; Uchida, S.; Grätzel, M. *Adv. Mater.* **2006,** *18*, 1202–1205.
(39) Huang, S. Y.; Schlichthörl, G.; Nozik, A. J.; Grätzel, M.; Frank, A. J. *J. Phys. Chem. B* **1997,** *101*, 2576–2582.
(40) Kern, R.; Sastrawan, R.; Ferber, J.; Stangl, R.; Luther, J. *Electrochim. Acta* **2002,** *47*, 4213–4225.
(41) Hagfeldt, A.; Grätzel, M. *Acc. Chem. Res.* **2000,** *33*, 269–277.
(42) Moser, J.; Punchihewa, S.; Infelta, P. P.; Grätzel, M. *Langmuir* **1991,** *7*, 3012–3018.
(43) Redmond, G.; Fitzmaurice, D. *J. Phys. Chem.* **1993,** *97*, 1426–1430.